Numerical solutions of the time-dependent Schrödinger equation: Reduction of the error due to space discretization

Hezhu Shao (邵和助)* and Zhongcheng Wang (汪仲诚)†

Department of Physics, Shanghai University, 99 Shangda Road, Shanghai 200444, People's Republic of China

(Received 30 November 2008; revised manuscript received 31 March 2009; published 21 May 2009)

We present an improved space-discretization scheme for the numerical solutions of the time-dependent Schrödinger equation. Compared to the scheme of W. van Dijk and F. M. Toyama [Phys. Rev. E **75**, 036707 (2007)], the present one, which contains more terms of second-order partial derivatives, greatly reduces the error resulting from the spatial integration. For a $(2l+1)$-point formula with $(2l+1)$ terms of second-order partial derivatives, the local truncation error can decrease from the order of $(\Delta x)^{2l}$ to $(\Delta x)^{4l}$, while the previous one contains only one term of second-order partial derivative. Two well-known numerical examples and the corresponding error analysis demonstrate that the present scheme has an advantage in the precision and efficiency over the previous one.

DOI: 10.1103/PhysRevE.79.056705 PACS number(s): 02.60.−x, 02.70.−c, 03.67.Lx, 03.65.−w

I. INTRODUCTION

The development of accurate and efficient integration methods for the time-dependent Schrödinger equation (TDSE) has received considerable attention in recent years because the solutions of the TDSE are instructive for gaining insight into the quantum behavior of the systems described by the TDSE in various fields of physics (see [1] and its references). In this paper, we consider the TDSE,

$$\left(i\hbar\frac{\partial}{\partial t}-H\right)\psi(x,t)=0,\quad \psi(x,t_0)=\phi(x), \tag{1}$$

where the operator H is a time-independent Hamiltonian,

$$H=-\frac{\hbar^2}{2m}\frac{\partial^2}{\partial x^2}+V(x), \tag{2}$$

and $\phi(x)$ is a given wave function at initial time t_0. The time evolution of the system described by Eq. (1) can be expressed in terms of an operator acting on the wave function at time t, which gives the wave function at a later time $t+\tau$, as

$$\psi(x,t+\tau)=e^{-iH\tau/\hbar}\psi(x,t). \tag{3}$$

The Crank-Nicolson (CN) implicit integration method has been widely used for solving Eq. (3) numerically because of its unitarity and unconditional stability. Whereas the CN method has low accuracy with an error of $\mathcal{O}(h^2,\tau^3)$, where h and τ are spatial and time step sizes, respectively, several authors have proposed some schemes to improve it. Mişicu *et al.* introduced a seven-point formula with an error of $\mathcal{O}(h^6)$ for the second-order spatial derivative and an improved time-integration scheme with an error of $\mathcal{O}(\tau^5)$ [2]. Moyer used a Numerov scheme for the spatial-integration method with an error of $\mathcal{O}(h^6)$ [3]. Puzynin *et al.* indicated how to generalize the time development to higher order [4,5]. Iitaka introduced an explicit scheme for the time evolution by extending the second-order difference scheme to fourth-, sixth-, and higher-order accuracy [6]. Dias *et al.* used a high-order method based on the Taylor expansion of the evolution operator to solve the time evolution of the wave function numerically [7]. Recently, van Dijk and Toyama (DT) put forward a $(2r+1)$-point formula for the second-order spatial derivative, which reduced the error in the integration over space on the order of $\mathcal{O}(h^{2r})$, and extended the work of Puzynin *et al.* on the Padé approximant method for the time evolution operator as well [1].

In this paper, we present an improved method of spatial integration for finding the numerical solution to the TDSE. We derive this scheme in Sec. II. In Sec. III, two numerical illustrations are presented and an example on error analysis for explaining the obtained results is provided and, in the final section, a summary is given.

II. DERIVATION

Following [1], we employ the Padé approximant in the calculation of the time evolution operator. The $[L/L]$ diagonal Padé approximant of the exponential function $e^{-i\epsilon}$ can be expanded as

$$e^{-i\epsilon}\approx\left(1+\sum_{n=1}^{L}\alpha_n(-i\epsilon)^n\right)/\left(1+\sum_{n=1}^{L}\alpha_n(i\epsilon)^n\right), \tag{4}$$

which can be further transferred into

$$e^{-i\epsilon}=(-1)^L\prod_{\nu=1}^{L}\frac{\epsilon+z_\nu^{(L)}}{\epsilon+\tilde{z}_\nu^{(L)}}, \tag{5}$$

where $\{z_1^{(L)},z_2^{(L)},\ldots,z_L^{(L)}\}$ are the roots of the denominator of the right-hand side of Eq. (4) and $\{\tilde{z}_1^{(L)},\tilde{z}_2^{(L)},\ldots,\tilde{z}_L^{(L)}\}$ are the complex conjugates of $\{z_1^{(L)},z_2^{(L)},\ldots,z_L^{(L)}\}$. The coefficients of Eq. (4) are identical with those obtained by the following Obrechkoff one-step difference equation [8,9]:

*hzshao@hotmail.com
†zc_wang89@hotmail.com

TABLE I. The coefficients $a_k^{(M)}$ and $c_k^{(M)}$ up to $M=4$.

M		$k=0$	1	2	3	4
1	$a_k^{(1)}$	1	$\frac{1}{10}$			
	$c_k^{(1)}$	$\frac{12}{5}$	$-\frac{6}{5}$			
2	$a_k^{(2)}$	1	$\frac{344}{1179}$	$\frac{23}{2358}$		
	$c_k^{(2)}$	$\frac{265}{131}$	$-\frac{320}{393}$	$-\frac{155}{786}$		
3	$a_k^{(3)}$	1	$\frac{329913}{725308}$	$\frac{18387}{362654}$	$\frac{619}{725308}$	
	$c_k^{(3)}$	$\frac{813155}{543981}$	$-\frac{263655}{725308}$	$-\frac{130977}{362654}$	$-\frac{49483}{2175924}$	
4	$a_k^{(4)}$	1	$\frac{1375194944}{2412048335}$	$\frac{271939448}{2412048335}$	$\frac{16267712}{2412048335}$	$\frac{330907}{4824096670}$
	$c_k^{(4)}$	$\frac{6442681595}{5788916004}$	$-\frac{115253824}{1447229001}$	$-\frac{580942096}{1447229001}$	$-\frac{105962944}{1447229001}$	$-\frac{25410683}{11577832008}$

$$y\left(x+\frac{h}{2}\right)-y\left(x-\frac{h}{2}\right)-\sum_{n=1}^{L}\alpha_n h^n \times\left[y^{(n)}\left(x+\frac{h}{2}\right)-(-1)^n y^{(n)}\left(x-\frac{h}{2}\right)\right]=E_{LT}(h), \quad (6)$$

where $E_{LT}(h)$ is the local truncation error. Expanding the left-hand side of Eq. (6) into a $(2L+1)$-order Taylor series and solving a system of linear equations, we can obtain the coefficients α_n $(n=1,2,\ldots,L)$ and the local truncation error,

$$E_{LT}(h)=(-1)^L\frac{h^{2L+1}y^{(2L+1)}(\xi)}{2^{2L}(2L-1)!\,!\,(2L+1)!\,!}, \quad (7)$$

where $x-h/2<\xi<x+h/2$. The time evolution operator in Eq. (3) can be expressed by the $[L/L]$ diagonal Padé approximant as

$$e^{-iH\tau/\hbar}=(-1)^L\prod_{\nu=1}^{L}K_\nu^{(L)}+\mathcal{O}(\tau^{2L+1}), \quad (8)$$

where

$$K_\nu^{(L)}=\frac{H+(\hbar/\tau)z_\nu^{(L)}}{H+(\hbar/\tau)\tilde{z}_\nu^{(L)}}. \quad (9)$$

Since the Hamiltonian H is time independent, the commutative relation $[K_\kappa^{(L)},K_\nu^{(L)}]=0$ holds. Using expression (8) in Eq. (3), we obtain

$$\psi(x,t_n+\tau)=(-1)^L\prod_{\nu=1}^{L}K_\nu^{(L)}\psi(x,t_n). \quad (10)$$

Defining

$$\psi\left(x,t_n+\frac{s}{L}\tau\right)=(-1)K_s^{(L)}\psi\left(x,t_n+\frac{s-1}{L}\tau\right), \quad (11)$$

one can solve for $\psi(x,t_n+\tau)$ recursively, starting with

$$\psi\left(x,t_n+\frac{1}{L}\tau\right)=(-1)K_1^{(L)}\psi(x,t_n). \quad (12)$$

As for the spatial integration, DT employed a $(2r+1)$-point formula for the second-order spatial derivative [1],

$$\frac{\partial^2}{\partial x^2}\psi(x,t)+\frac{1}{h^2}\sum_{k=-r}^{r}c_k^{(r)}\psi(x+kh,t)=\mathcal{O}(h^{2r}). \quad (13)$$

We use the following $(2M+1)$-point difference formula, in which we take full advantage of second-order partial derivatives of the wave function and the wave function itself as well, to improve the DT scheme,

$$\frac{\partial^2}{\partial x^2}\sum_{k=-M}^{M}a_k^{(M)}\psi(x+kh,t)+\frac{1}{h^2}\sum_{k=-M}^{M}c_k^{(M)}\psi(x+kh,t)=E_{LT}(h), \quad (14)$$

where we set $a_0^{(M)}=1$. By letting all of $a_k^{(M)}$ be zero except for $k=0$, one would reduce Eq. (14) to the DT scheme. By making expansions of the left-hand side of Eq. (14) with Taylor series to the order of $\mathcal{O}(h^{4M-2})$, one would obtain $2M+1$ associate equations and determine the coefficients $a_{-M}^{(M)},\ldots,a_M^{(M)}$ and $c_{-M}^{(M)},\ldots,c_M^{(M)}$ by solving these equations. Because Eq. (14) is invariant under the change of h to $-h$, the coefficients satisfy the relation $\{a_{-k}^{(M)},c_{-k}^{(M)}\}=\{a_k^{(M)},c_k^{(M)}\}$ for $k=1,2,\ldots,M$. For example, the coefficients for $M=1,2,\ldots,4$ are given in Table I. From Eqs. (9) and (11), we have

$$\left(H+\frac{\hbar}{\tau}\tilde{z}_s^{(L)}\right)\psi\left(x+kh,t_n+\frac{s}{L}\tau\right)=(-1)\left(H+\frac{\hbar}{\tau}z_s^{(L)}\right)\psi\left(x+kh,t_n+\frac{s-1}{L}\tau\right) \quad (15)$$

for $k=0,\pm1,\pm2,\ldots,\pm M$. Multiplying both sides of Eq. (15) by $a_k^{(M)}$ for $k=0,\pm1,\pm2,\ldots,\pm M$ and adding the $2M+1$ equations, we have

$$\sum_{k=-M}^{M} a_k^{(M)}\left(H+\frac{\hbar}{\tau}\tilde{z}_s^{(L)}\right)\psi\left(x+kh,t_n+\frac{s}{L}\tau\right)$$
$$=(-1)\sum_{k=-M}^{M} a_k^{(M)}\left(H+\frac{\hbar}{\tau}z_s^{(L)}\right)\psi\left(x+kh,t_n+\frac{s-1}{L}\tau\right). \quad (16)$$

Remembering

$$H\psi(x,t)\rightarrow -\frac{\hbar^2}{2m}\frac{\partial^2}{\partial x^2}\psi(x,t)+V(x)\psi(x,t), \quad (17)$$

and denoting $v(x)=2mV(x)(h/\hbar)^2$ and $\mu=2mh^2/\hbar$, we rewrite Eq. (16) as

$$\sum_{k=-M}^{M}\left\{-h^2a_k^{(M)}\frac{\partial^2}{\partial x^2}+a_k^{(M)}\left[v(x+kh)+\frac{\mu}{\tau}\tilde{z}_s^{(L)}\right]\right\}$$
$$\times\psi\left(x+kh,t_n+\frac{s}{L}\tau\right)=(-1)\sum_{k=-M}^{M}$$
$$\times\left\{-h^2a_k^{(M)}\frac{\partial^2}{\partial x^2}+a_k^{(M)}\left[v(x+kh)+\frac{\mu}{\tau}z_s^{(L)}\right]\right\}$$
$$\times\psi\left(x+kh,t_n+\frac{s-1}{L}\tau\right). \quad (18)$$

Using Eq. (14) to eliminate the second-order partial derivatives in the two sides of Eq. (18), we have

$$\sum_{k=-M}^{M}\left\{c_k^{(M)}+a_k^{(M)}\left[v(x+kh)+\frac{\mu}{\tau}\tilde{z}_s^{(L)}\right]\right\}\psi\left(x+kh,t_n+\frac{s}{L}\tau\right)$$
$$=(-1)\sum_{k=-M}^{M}\left\{c_k^{(M)}+a_k^{(M)}\left[v(x+kh)+\frac{\mu}{\tau}z_s^{(L)}\right]\right\}$$
$$\times\psi\left(x+kh,t_n+\frac{s-1}{L}\tau\right). \quad (19)$$

We assemble the wave function as a vector

$$\Psi_n=\{\psi_{0,n},\psi_{1,n},\ldots,\psi_{j,n},\ldots,\psi_{J,n}\} \quad (20)$$

for the time $t_n=t_0+n\tau$ $(n=0,1,\ldots,N)$, where the component $\psi_{j,n}$ is for $x_j=x_0+jh$ $(j=0,1,\ldots,J)$, and assume $\psi_{j,n}=0$ for anytime with $x<x_0$ and $x>x_J$. Then Eq. (19) can be rewritten as the matrix equation

$$(B_s^{(L)})^*\Psi_{n+s/L}=(-1)B_s^{(L)}\Psi_{n+(s-1)/L}, \quad (21)$$

where $B_s^{(L)}$ is a $(2M+1)$-diagonal matrix and the matrix $(B_s^{(L)})^*$ is the complex conjugate of matrix $B_s^{(L)}$. The elements of matrix $B_s^{(L)}$ are given by

$$b_{j,j\pm k}^{(L,s)}=c_k^{(M)}+a_k^{(M)}\left(v_{j\pm k}+\frac{\mu}{\tau}z_s^{(L)}\right). \quad (22)$$

We employ the LU decomposition [10], which writes the matrix $(B_s^{(L)})^*$ of the left-hand side of equation (21) as the product of a lower triangular matrix and an upper triangular matrix, to solve the matrix equation (21).

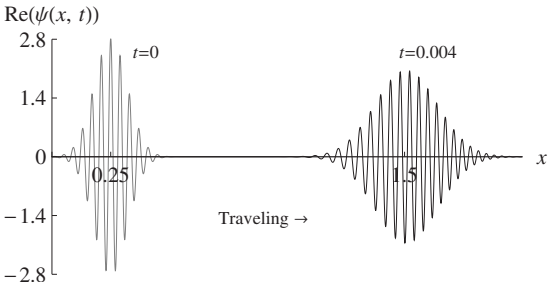

FIG. 1. The real part of wave packet described by Eq. (24).

III. RESULTS AND DISCUSSION

In this section, we use two examples and an error analysis to evaluate the precision and efficiency of our present method.

A. Propagation of a wave packet

The first example is to solve the problem of the propagation of free-particle wave packets [1,11]. The free wave-packet propagation with its initial wave function,

$$\psi(x,0)=(2\pi\sigma_0^2)^{-1/4}e^{ik_0(x-x_0)}e^{-(x-x_0)^2/(2\sigma_0)^2}, \quad (23)$$

has the following analytical solution:

$$\psi(x,t)=(2\pi\sigma_0^2)^{-1/4}[1+i\hbar t/(2m\sigma_0^2)]^{-1/2}$$
$$\times\exp\left(\frac{-(x-x_0)^2/(2\sigma_0)^2+ik_0(x-x_0)-i\hbar k_0^2t/(2m)}{1+i\hbar t/(2m\sigma_0^2)}\right). \quad (24)$$

We set $\hbar=1$, $m=1/2$, $\sigma_0=1/20$, $k_0=50\pi$, and let the packet travel from $t_0=0$, with its center at 0.25 to the destination time $t_d=0.004$, with its center at 1.5 as shown in Fig. 1. To reduce the error for the normalization of the packet, the range of spatial integration is set from −0.75 to 3.25. We use the DT method and our present method to calculate the wave function under the following conditions:

(1) $L=10$ with the time step size τ from 0.000 026 666 7 to 0.0008 and

(2) $M=r=6$, 8, and 10 with the spatial step size $h=0.012$, 0.01, 0.008, and 0.006.

We calculate the magnitude of error by comparing the obtained $\psi(x,t_d)$ with the analytical one using the formula [4]

$$e_1=\max_x|\psi(x,t_d)-\psi_{exact}(x,t_d)|. \quad (25)$$

The numerical results for errors and CPU run time [12] as a function of τ are summarized in Figs. 2 and 3, where the lines of A1 (blue empty circle), A2 (blue empty square), A3 (blue empty diamond), and A4 (blue empty triangle) are obtained by the DT method with the spatial step sizes of $h=0.012$, 0.01, 0.008, and 0.006, respectively, and B1 (red filled circle), B2 (red filled square), B3 (red filled diamond), and B4 (red filled triangle) by our present method with the same respective values of spatial step size as those employed in the DT method. For the cases of $\{M=r=10$, $h=0.008$ and

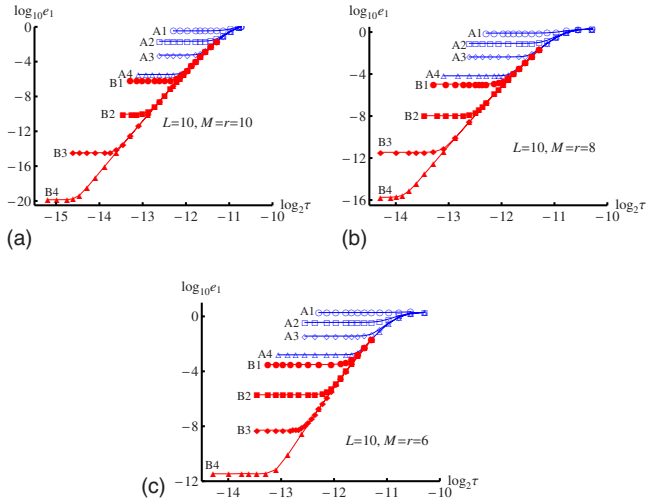

FIG. 2. (Color online) The logarithm of e_1 to the base 10, plotted as a function of the logarithm of τ to the base 2, for the propagation of a wave packet with $L=10$ and (a) $M=r=10$, (b) $M=r=8$, and (c) $M=r=6$.

0.006} [B3 and B4 in Fig. 2(a)] and {$M=r=8$, $h=0.006$} [B4 in Fig. 2(b)], we use a modern computational software packages of MATHEMATICA for multiple precision calculations [13] considering the results would be reaching an accuracy of equal to or less than 10^{-16}, which is the standard precision in most computing systems. From Figs. 2 and 3, we conclude that:

(1) The error is not affected by the change in the time step size τ within a certain range; nevertheless, the logarithm of e_1 to the base 10 approaches an asymptote when τ becomes larger.

(2) For the cases of $M=r$ and same $\{L,h,\tau\}$, the two methods take almost the same CPU run time as shown in Figs. 3(a) and 3(b) and, compared to the DT method, our present method can improve the accuracy dramatically: for some cases it increases about 9 orders of magnitude; for examples, {$h=0.01$, $M=r=10$} [A2 and B2 in Fig. 2(a)], {$h=0.008$, $M=r=8$} [A3 and B4 in Fig. 2(b)], and {$h=0.006$, $M=r=6$} [A4 and B4 in Fig. 2(c)]. For the extreme case of

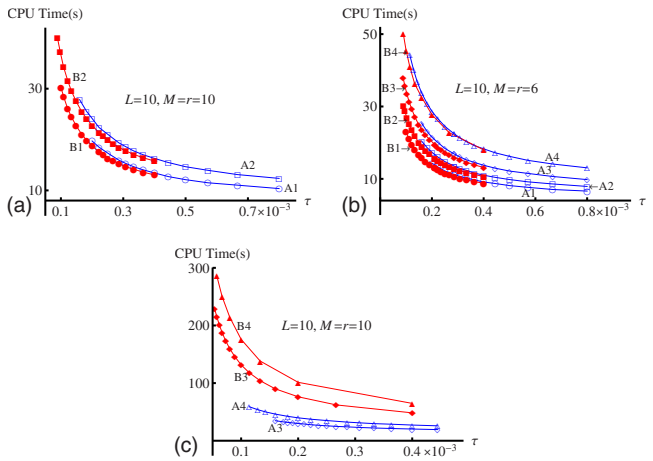

FIG. 3. (Color online) The CPU time(s), plotted as a function of τ.

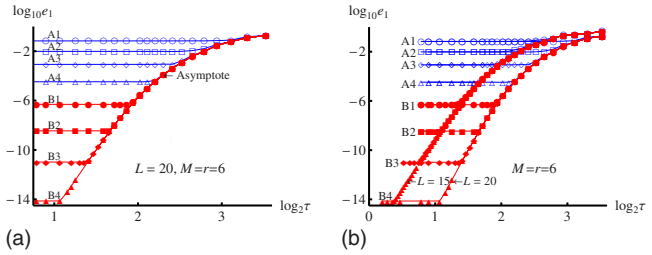

FIG. 4. (Color online) The logarithm of e_1 to the base 10, plotted as a function of the logarithm of τ to the base 2, for the oscillation of a coherent wave packet with the parameters of $M=r=6$ and (a) $L=20$ and (b) $L=20$ and 15.

{$h=0.006$, $M=r=10$} [A4 and B4 in Fig. 2(a)], it has improved by about 14 orders of magnitude.

(3) From Fig. 3(c), we see that the calculation with the same parameters $\{L,h,\tau\}$ and $M=r$ with multiple precisions would take almost three times the CPU run time as that under the floating precision.

B. Oscillation of a coherent wave packet

The TDSE of the oscillation of a coherent state for the harmonic oscillator is

$$i\hbar\frac{\partial}{\partial t}\psi(x,t)=\left(-\frac{\hbar^2}{2m}\frac{\partial^2}{\partial x^2}+\frac{1}{2}Kx^2\right)\psi(x,t). \tag{26}$$

The time evolution of the oscillation of coherent states has been discussed recently in connection with the quantum abacus [14]. The exact expression for the time-dependent wave function [15] can be written as

$$\psi_{exact}=\frac{\alpha^{1/2}}{\pi^{1/4}}\exp\left[-\frac{1}{2}(\xi-\xi_0\cos\omega t)^2-i\left(\frac{1}{2}\omega t+\xi\xi_0\sin\omega t-\frac{1}{4}\xi_0^2\sin 2\omega t\right)\right], \tag{27}$$

where the time evolution of the initially displaced ground-state wave function is considered,

$$\psi(x,0)=\frac{\alpha^{1/2}}{\pi^{1/4}}e^{(-1/2)\alpha^2(x-a)^2}, \tag{28}$$

with $\alpha^4=mK/\hbar^2$, $\xi=\alpha x$, $\xi_0=\alpha a$, and $\omega=\sqrt{K/m}$. We set $m=1$, $\hbar=1$, $a=10$, and $\omega=1/5$. Apart from the phase factor $e^{-i\omega t/2}$, the period of oscillation is 10π. We use the two schemes to calculate the wave function from $t=0$ to $t_d=11T=110\pi$, as van Dijk and Toyama chose in [1], and the spatial domain $x\in[x_0,x_J]=[-30,30]$ under the following conditions:

(1) $L=20$ and 15 with the time step size τ from $110\pi/300$ to $110\pi/30$ and

(2) $M=r=6$ with $h=0.3$, 0.4, 0.5, and 0.6.

The numerical results of the logarithm of e_1 to the base 10 as a function of the logarithm of τ to the base 2 are summarized in Fig. 4, where the lines of A1 (blue empty circle), A2 (blue empty square), A3 (blue empty diamond), and A4 (blue empty triangle) are calculated by the DT method with the

spatial step size of $h=0.6$, 0.5, 0.4, and 0.3, respectively, and B1 (red filled circle), B2 (red filled square), B3 (red filled diamond), and B4 (red filled triangle) by our present method with the same respective spatial step sizes as those chosen in the DT method. For the cases of $\{M=r=6, h=0.3, L=20$ and $15\}$ (B4 in Fig. 4), we use the multiple precisions. Figure 4(a) shows that our present method surpasses the DT method by about 5 and 10 orders of magnitude when $M=r=6$ is used with the spatial step size $h=0.6$ and $h=0.3$, respectively. From Fig. 4, we can also see that the logarithm of e_1 to the base 10 approaches an asymptote as τ becomes larger and the asymptote will move toward the larger time step size τ when the higher-order Padé approximant is employed.

C. Error analysis

The above examples show that the numerical precision for the TDSE is not affected by the change in τ or the order parameters of the Padé approximant method within a certain range. In what follows we shall investigate the source of the error in the framework of the space discretization and the Padé approximant method for the time evolution operator and explain the interesting findings obtained in the calculation.

In the following discussion, we set $\hbar=1$. Denoting δH as the error resulting from the space discretization, which should be a function of the spatial step size h, we can separate the Hamiltonian H in Eq. (3) into H_0, which is employed in the calculation, and δH. For the final time $t_d=t_0+n\tau$, Eq. (3) becomes

$$\psi(x,t_d)=\psi(x,t_0+n\tau)=[\exp(-iH_0\tau)\exp(-i\delta H\tau)]^n\psi(x,t_0). \tag{29}$$

On the other hand, $[\exp(-i\delta H\tau)]^n\approx 1-in\delta H\tau$ for the case $n\delta H\tau\ll 1$ and $\exp(-iH_0\tau)$ can be expressed into the sum of $M(H_0,\tau)$ and an error $\Delta M(H_0,\tau)$, and $\Delta M(H_0,\tau)/M(H_0,\tau)\ll 1$, so

$$[\exp(-iH_0\tau)]^n=[M(H_0,\tau)+\Delta M(H_0,\tau)]^n\approx M(H_0,\tau)^n + n\Delta M(H_0,\tau)M(H_0,\tau)^{n-1}. \tag{30}$$

Hence, regardless of the higher-order infinitesimal, $\psi(x,t_d)$ can be approximately expressed as

$$[M(H_0,\tau)^n+nM(H_0,\tau)^{n-1}\Delta M(H_0,\tau) - iM(H_0,\tau)^n n\tau\delta H]\psi(x,t_0), \tag{31}$$

where $M(H_0,\tau)^n\psi(x,t_0)$ and $M(H_0,\tau)^{n-1}\psi(x,t_0)$ are just the numerical wave functions of $\psi(x,t_d)$ and $\psi(x,t_d-\tau)$. Denoting the error of the calculated wave function as $\max_x|\psi(x,t_d)-\psi_{exact}(x,t_d)|$ according to Eq. (25), we obtain the error

$$e_t=\max_x\left|\frac{\Delta M(H_0,\tau)}{\tau}(t_d-t_0)\psi(x,t_d-\tau) + (-i\delta H)(t_d-t_0)\psi(x,t_d)\right|. \tag{32}$$

Assuming $\max_x|\psi(x,t_d-\tau)|\simeq\max_x|\psi(x,t_d)|$, Eq. (32) can be simplified to

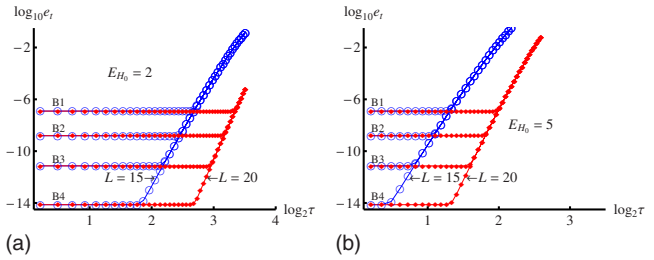

FIG. 5. (Color online) The logarithm of e_t to the base 10, plotted as a function of logarithm of τ to the base 2, for the diagonal Padé approximant of [15,15] and [20,20], which are denoted by $L=15$ (blue empty circle) and $L=20$ (red filled diamond), respectively, in which (a) $E_{H_0}=2$ and (b) $E_{H_0}=5$.

$$e_t=(t_d-t_0)\max_x|\psi(x,t_d)|\sqrt{\left(\frac{\Delta M(H_0,\tau)}{\tau}\right)^2+(\delta H)^2}. \tag{33}$$

In the following, we will compare the calculated e_1 as shown in Fig. 4 with the error e_t predicted by Eq. (33). Since δH is the error due to discretization of space, it should be $\mathcal{O}(h^{4M})$ for the $(2M+1)$-point formula in our present method. Thus we set

$$\delta H=P_s h^{4M}, \tag{34}$$

where the parameter P_s is dependent on the order of spatial-integration method. When $H_0\tau\ll 1$, $\Delta M(H_0,\tau)/\tau=P_t H_0(H_0\tau)^{2L}$ according to Eq. (7), where the parameter P_t is dependent on the order of the Padé approximant. If $H_0\tau\geq 1$, we should express $\Delta M(H_0,\tau)$ as

$$\Delta M(H_0,\tau)=\left|\exp(-iE_{H_0}\tau)-(-1)^L\prod_{\nu=1}^{L}K_\nu^{(L)}(E_{H_0})\right|, \tag{35}$$

where E_{H_0} is used to represent the energy level of the system. In the second problem we have tested, $|(t_d-t_0)\max_x\psi(x,t_d)|=|(110\pi-0)0.5023|=173.58$ and $e_1=7.38\times 10^{-15}$ when $M=r=6$ and $\{L,h,\tau\}=\{20,0.3,11\pi/20\}$ are employed, so we have

$$P_s=\frac{7.38\times 10^{-15}}{173.58\times 0.3^{24}}=0.00015. \tag{36}$$

According to expressions (34) and (36), we obtain the errors from the spatial integration to be 7.35×10^{-12}, 1.56×10^{-9}, and 1.24×10^{-7} for the spatial step sizes $h=0.4$, $h=0.5$, and $h=0.6$, respectively, which agree with the calculations as shown in Fig. 4. If a is large, according to [15], the energy level E_{H_0} is approximately equal to $\frac{1}{2}Ka^2$ while $E_{H_0}=\frac{1}{2}KA_0^2$ from the classical point of view and A_0 is the amplitude of the oscillator, then $E_{H_0}=2$. The practical amplitude of the oscillator is greater than a. We plot $\log_{10} e_t$ in Fig. 5 according to Eqs. (33)–(36) with $L=15$ and 20, where the estimated energy $E_{H_0}=2$ and 5 are used for Figs. 5(a) and 5(b). Comparing Fig. 5 with Fig. 4(b), we can see that Fig. 5(b) is in better agreement with Fig. 4(b) than Fig. 5(a), which means

the energy value of the system approximates 5 and the corresponding classical amplitude $A_0 \simeq 15.8114$. From the above error analysis, we can immediately draw the following points:

(1) the error δH, which is ascribed to the space discretization, plays a primary role when the time step size τ is small; however, $\Delta M(H_0, \tau)/\tau$ resulted from the Padé approximant method for the time evolution operator will be the leading error as τ gradually increases and

(2) the higher-order Padé approximant leads to the larger domains of the time step size τ, in which δH is the primary error.

IV. SUMMARY

By two well-known numerical examples, we demonstrate that the present space-discretization scheme presented in this paper greatly improve the spatial integration giving many orders of magnitude improvement in the precision of the results. This method should be a significant tool for solving the time-dependent Schrödinger equation.

ACKNOWLEDGMENTS

We wish to thank an anonymous referee for carefully reading the manuscript and for constructive comments and suggestions. We wish to acknowledge the support from Project Grant No. A.10-0101-06-426 by the Shanghai Education Committee. We also wish to acknowledge the support of the Department of Physics, Shanghai University.

[1] W. van Dijk and F. M. Toyama, Phys. Rev. E **75**, 036707 (2007).
[2] Ş. Mişicu, M. Rizea, and W. Greiner, J. Phys. G **27**, 993 (2001).
[3] C. A. Moyer, Am. J. Phys. **72**, 351 (2004).
[4] I. Puzynin, A. Selin, and S. Vinitsky, Comput. Phys. Commun. **123**, 1 (1999).
[5] I. Puzynin, A. Selin, and S. Vinitsky, Comput. Phys. Commun. **126**, 158 (2000).
[6] T. Iitaka, Phys. Rev. E **49**, 4684 (1994).
[7] W. S. Dias, E. M. Nascimento, M. L. Lyra, and F. A. B. F. de Moura, Phys. Rev. B **76**, 155124 (2007).
[8] Z. Wang and Q. Chen, Comput. Phys. Commun. **170**, 49 (2005).
[9] H. Shao and Z. Wang, Comput. Phys. Commun. **180**, 1 (2009).
[10] W. H. Press, S. A. Teukolsky, W. T. Vetterling, and B. P. Flannery, *NUMERICAL RECIPES: The Art of Scientific Computing*, 3rd ed. (Cambridge University Press, Cambridge, England, 2007).
[11] A. Goldberg, H. M. Schey, and J. L. Schwartz, Am. J. Phys. **35**, 177 (1967).
[12] The CPU time is a relative measure. The calculations of Fig. 3 were done on a PC with AMD Athlon(tm) 64 processor 2800 + 1.80 GHz 512 M memory.
[13] S. Wolfram, *The Mathematica Book*, 5th ed. (Wolfram Media, Champaign, IL, 2003).
[14] T. Cheon, I. Tsutsui, and T. Fülöp, Phys. Lett. A **330**, 338 (2004).
[15] L. I. Schiff, *Quantum Mechanics*, International Series in Pure and Applied Physics, 1st ed. (McGraw-Hill Book Company Inc., New York, 1949).